Seasonal dynamics of phytoplankton and Calanus finmarchicus in the North Sea as revealed by a coupled one-dimensional model

Francois Carlotti, Günther Radach

Limnol. Oceanogr., 41(3), 1996, 522–539

Seasonal dynamics of phytoplankton and *Calanus finmarchicus* in the North Sea as revealed by a coupled one-dimensional model

François Carlotti
Station Zoologique, URA CNRS 716, BP 28, F-06230 Villefranche-sur-Mer, France

Günther Radach
Institut für Meereskunde, Troplowitzstr. 7, 22529 Hamburg, Germany

Abstract

A population dynamics model for *Calanus finmarchicus* was coupled with a one-dimensional physical and biological upper layer model for phosphate and phytoplankton to simulate the development of the successive stages of *Calanus* and study the role of these stages in the dynamics of the northern North Sea ecosystem. The copepod model links trophic processes and population dynamics, and simulates individual growth within stages and the changes in biomass between stages.

Simulations of annual cycles contain two or three generations of *Calanus* and indicate the importance of growth of late stages to total population biomass. The spring peak of zooplankton lags that of phytoplankton by a month due to growth of the first cohort. When compared with observations, the simulation shows a broad phytoplankton bloom and a low biomass of *Calanus*. A higher initial overwintering stock changes the dynamics of *Calanus*, but not the annual biomass. The timing of the spring ascent of overwintering individuals influences subsequent dynamics.

Simulations of spring dynamics compared with data obtained during the Fladen Ground Experiment in 1976 show that grazing by *Calanus* cannot be the only major cause limiting the phytoplankton bloom because development of the first stages of *Calanus* is slow, and the last copepodite stages arrive after the bloom. *Calanus* never attains realistic biomasses feeding on phytoplankton as a single food source. These simulations led us to add a compartment of pelagic detritus, which provides another food source to enable *Calanus* population growth.

The interactions between physical and biological processes are an important part of planktonic ecosystem dynamics; however, studying these processes simultaneously often is difficult because of different time and space scales (Mar. Zooplankton Colloq. 1 1989). During the last decade, several workers (e.g. Mullin et al. 1985; Wroblewski and Richmann 1987; Kiørboe and Nielsen 1990) have demonstrated the important role of physical mixing on temporal scales of from a few days to several years for primary and secondary production. Primary production depends mainly on the stability of the water column; strong vertical mixing initially reduces production but supplies the upper water column with nutrients and thereby stimulates subsequent production. Not only is copepod production considered dependent on phytoplankton production, but these dynamics over small time and space scales may also attenuate trophic variability, ultimately affecting the relationship between primary production and fisheries (Runge 1988). Events such as storms or intense heating may have severe consequences for the structure of the whole food chain, including fish recruitment (Mullin et al. 1985).

Our understanding of the role that time-limited events play in long-range ecosystem dynamics is largely based on dynamics simulations with mixed-layer models that couple nutrient and plankton dynamics (*see* Fransz et al. 1991*b*). However, most of these models take into account only nutrients and phytoplankton (Fransz et al. 1991*b*), probably because of the difficulty of representing the complex behavior that exists among zooplankton species and also among the different zooplankton developmental stages. Models having one compartment for the whole zooplankton community are useful only for simulating ecosystem dynamics over the course of a few days (Wroblewski and Richman 1987) or for a stable environment but become meaningless for long periods if the environment fluctuates. Although field workers consider population dynamics to be the minimum level of study, zooplankton population models are rarely included in ecosystem models. Steele and Henderson (1976) demonstrated that a comprehensive model of the North Sea food chain needs to take into account the population dynamics of *Calanus finmarchicus*. Our goal is to define how and when such coupling of phytoplankton and zooplankton is truly necessary. As an example, we use *C. finmarchicus* in the North Sea; this species dominates the biomass of zooplankton in spring and summer and shows clearly

Acknowledgments

This work was completed while F.C. was a postdoctoral fellow at the Institut für Meereskunde der Universität Hamburg and was supported by a research stipend of Alexander von Humboldt Stiftung and by a fellowship from the STEP program of EEC. CNRS/INSU and URA 716 allowed F.C. to work in Hamburg in 1992.

We thank Andreas Moll for advice and Ortrud Kleinow and Matthias Regener for computer programming assistance. We also thank the anonymous reviewers and B. P. Boudreau and J. Dolan for comments and suggestions that helped to clarify the manuscript.

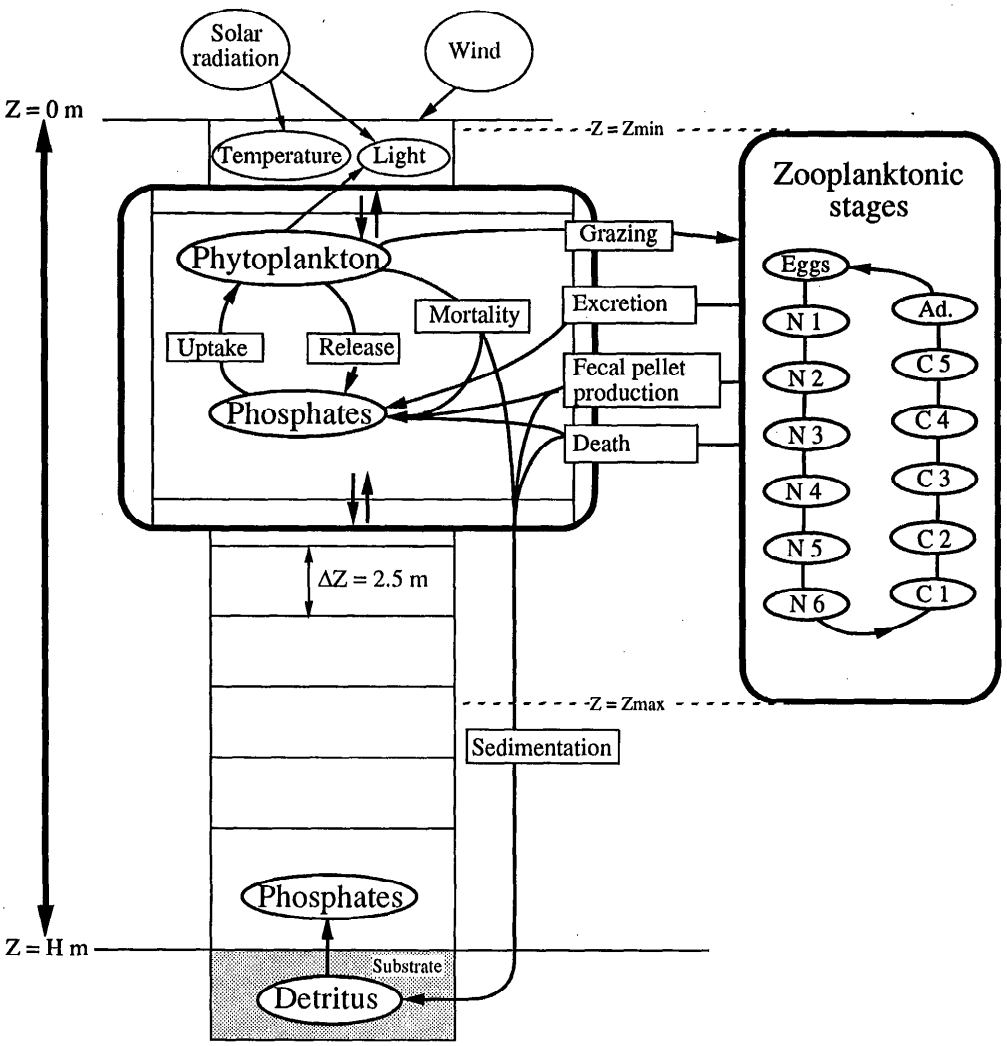

Fig. 1. Conceptual diagram of the coupled model. A stage dynamics model for *Calanus finmarchicus,* evenly distributed within a given layer, has been coupled with a 1-D vertically resolved physical and biological model. The physical submodel drives the dynamics of nutrients, phytoplankton, and benthic detritus. Formulations of processes are detailed by Radach and Moll (1993). Processes coupling the population of copepods to the ecosystem are given in Table 2.

demarcated cohorts. In fall, other species, such as *Centropages typicus,* take its place (Fransz et al. 1991*a*).

Recently, Radach and Moll (1993) developed a one-dimensional (1-D) physical and biological upper-layer model. This model simulates the annual cycles of the physical dynamics in the water column and the biological dynamics of phytoplankton and phosphate and estimates annual primary production in the central North Sea. Radach and Moll correlated these results with meteorological observations and estimated radiation data spanning 25 yr and clearly demonstrated the role played by short-term events in integrated annual production. In Radach and Moll's model, zooplankton were a forcing variable. In our paper, we combined their model with a population dynamics model for *C. finmarchicus,* similar to that described by Carlotti and Nival (1992). These two models have been independently calibrated and validated.

The model

Concept of the coupled model—We searched for the simplest model to explain the main features of plankton dynamics, including the dynamics of *C. finmarchicus* in the central and northern North Sea. Because the system is nonlinear, we deliberately did not choose the most complete but most complex model. Instead, we kept the structure of both simple submodels (Fig. 1) and added a "compartment" for pelagic detritus, which was not previously represented.

Radach and Moll's (1993) model consists of three submodels: a meteorological submodel that drives both a 1-D vertical submodel for the physics of the upper layer and a biological submodel, which also is driven by output from the physical model. We do not discuss the meteorological and physical submodels (*see* Radach and Moll 1993), but focus on the biological submodel. This submodel describes nutrient and phytoplankton dynamics in the water column and benthic deposition of detritus. Phytoplankton development depends on the supply of light and nutrients. Self-shading is also represented in the model. Phytoplankton produce new biomass, release catabolic substances, are affected by turbulent diffusion and sinking, and are either grazed on by zooplankton or deposited on the seabed. In the phytoplankton submodel, organic detritus in the water column is either immediately remineralized or directly transported to the bottom, where it accumulates in a stock of benthic detritus. The pool of nutrients is enriched in many ways: through benthic regeneration and turbulent diffusion; remineralization of dead phytoplankton, dead copepods, and fecal pellets; release from phytoplankton cells; and zooplankton excretion. The benthic detritus pool receives a flux of dead phytoplankton, fecal pellets, and dead zooplankton from the entire water column. Part of this detritus is remineralized in the water column, producing regenerated nutrients. The equations for the model are given by Radach and Moll (1993).

The copepod submodel can be divided into two levels: the first corresponds to the developmental instars (eggs, nauplii, copepodites, and adults), and the second is concerned with the age classes in each stage. In each age class, the variations of mean individual weight and the numbers of individuals are calculated as a function of various linked biological processes according to the conceptual model presented by Carlotti and Sciandra (1989, their figure 1). The growth rate and weight govern the processes of natural mortality, molting, and egg production. The model was conceived originally for *Euterpina acutifrons*, a small copepod without reserves. In our model of *C. finmarchicus*, we did not represent the accumulation of reserves because the North Sea population has a low fat content (except for overwintering individuals) compared to populations that stay in the North Atlantic (Carlotti et al. 1993).

Adaptation of the submodel to Calanus finmarchicus—Previously, we showed (Carlotti and Sciandra 1989; Carlotti and Nival 1992) that the zooplankton submodel can represent some fundamental functional relationships between the level of individuals and the level of the population. The mathematical formulations of the processes were presented by Carlotti and Sciandra (1989, their table 1).

The only changes we made to Carlotti and Sciandra's model was to the function f1—the dependence of the ingestion rate on the food concentration—and we adopted the double rectilinear model of Gamble (1978) rather than use the Ivlev-Parsons relationship (Carlotti and Sciandra 1989). The parameters of this function are the maximal ingestion rate (P1), the minimal threshold food concentration (P2), and the optimal food concentration (P3) that maximizes grazing rate. The values for all parameters are given in Table 1. The ingestion rate depends on the developmental stage, food supply, temperature, and weight of the animals. The first two naupliar stages of *C. finmarchicus* are unable to ingest particles; they are considered to live on reserves provided by the egg (Corner et al. 1967). For the other naupliar stages, we have the results of Fernandez (1979, his figure 3), who obtained maximum grazing rates of 0.4, 0.6, 1.0, and 1.5 μg C ind^{-1} d^{-1}, respectively, for N3–N6 of *C. pacificus* at 15°C. Naupliar grazing rates at 8°C were deduced from a function of temperature and are explained below. Daro (1980) estimated the maximal ingestion rates at 8°C during the Fladen Ground Experiment in 1976 (FLEX'76) to be 1, 5, 10, 15, and 20 μg C ind^{-1} d^{-1}, respectively, for C1–C5; Gamble (1978) estimated 25 μg C female^{-1} d^{-1}. The values of P1 are deduced by dividing these values by the body weight at 8°C. The threshold food concentration (P2) is equal to 50 μg C liter^{-1} for copepodite and adult stages (Daro 1980; Gamble 1978), but we chose a lower threshold of 20 μg C liter^{-1} for nauplii (Mullin and Brooks 1976; Fernandez 1979). The optimal food concentration (P3) for which ingestion is maximal also increases with each stage (Mullin and Brooks 1976). During FLEX'76, Gamble (1978) and Daro (1980) obtained a value of 150 μg C liter^{-1} for copepodites and adults. We fixed the value of P3 for the nauplii at 100 μg C liter^{-1}.

We use a value of 2.1 for Q_{10}, which is the value estimated by Gamble (1978) for *C. finmarchicus* in the North Sea; consequently, our parameter P5 has a value of 1.077. Because ingestion rates at 8°C act as our reference, the function f2 is equal to 1 at 8°C, and P4 is therefore equal to 0.476. The coefficient of allometry (P6), which relates ingestion to weight, is set to 0.7 (Paffenhöfer 1971). The assimilation rate (P7) of *Calanus* copepodites is ~70% (Gamble 1978). We assume that the assimilation rates of nauplii are slightly lower than those of copepodites. Respiration rates of naupliar and copepodite stages differ significantly (Marshall and Orr 1958), as do excretion rates (Corner et al. 1967, their figure 2). To approximate the values from Marshall and Orr (1958), nauplii would need to consume 20% of their weight for basic metabolism, and their active metabolism would have to correspond to 30% of their ingestion of carbon organic matter. N1 and N2, which do not feed, are assumed to consume 30% of their weight per day. For copepodites and adults, we attribute a minimum respiration rate of 4% of their weight per day, to which is added a respiration rate equal to 20% of the ingestion rate from C1 to C3 and 2% of the ingestion rate from C4 to adults. The effect of temperature on excretion operates through its effect on ingestion. Mullin and Brooks (1970*a*) showed that under the conditions of their experiments, the effects of temperature were equal, so the same fraction of ingested carbon appears as growth.

Carlotti et al. (1993) observed a temperature-dependent effect on the body weight of successive stages in *C. finmarchicus*. We use their empirical temperature-depen-

Table 1. Parameters used in the zooplankton submodel. Nondimensional—nd. Arrows indicate same value as to the left.

Parameters	Definitions	Eggs	N1	N2	N3	N4	N5	N6	C1	C2	C3	C4	C5	Adults
Ingestion														
P1	Max ingestion rate at 8°C, d^{-1}	0	0	0	1.5	←	2	←	←	←	←	←	←	←
P2	Limit of food concn, μg C $liter^{-1}$				20	←	←	←	50	←	←	←	←	←
P3	Optimal food concn, μg C $liter^{-1}$				100	←	←	←	150	←	←	←	←	←
P4	Temp. coeff., nd				0.476	←	←	←	←	←	←	←	←	←
P5	Temp. coeff., nd				1.077	←	←	←	←	←	←	←	←	←
P6	Exponent of allometric relation, nd				0.70	←	←	←	←	←	←	←	←	←
Egestion														
P7	Assimilation efficiency, nd				0.60	←	←	←	0.70	←	←	←	←	←
Excretion														
P8	Routine excretion rate, d^{-1}		0.30	←	0.20	←	←	←	0.04	←	←	←	←	←
P9	Coeff. of proportionality, nd		0	←	0.30	←	←	←	0.20	←	←	0.02	←	←
Reproduction														
P10	Asymptote of reproduction function, μg C ind^{-1} d^{-1}													40
P11	Exponent, nd													5
X13	Critical wt for maturation at 8°C, μg C													110
Mortality														
P12	Threshold of specific budget, d^{-1}				0.1	←	←	←	←	←	←	←	←	←
P13	Shape factor, d^{-1}				0.05	←	←	←	←	←	←	←	←	←
P14	Max rate, d^{-1}	0.05	←	←	0.10	←	←	←	←	←	←	←	0.05	←
P15	Min, d^{-1}				0.04	←	←	0.08	0.02	←	←	←	←	←
Transfer														
P16	Exponent, nd				30	←	←	←	←	←	←	←	←	
Xi	Critical molting wt at 8°C, μg C				0.4	0.6	0.8	1.1	2.5	7	15	40	90	
P17	Coeff. of proportionality, d^{-1}				7.0	←	←	←	←	←	←	←	←	
Hatching and molting of N1 and N2														
P18	Fitted parameter, nd	691	←	←										
P19	Shape factor, nd	−2.05	←	←										
P20	Temp. of reference, °C	10.26	←	←										

dent functions obtained from *C. finmarchicus* data in the North Sea. Critical weights at 8°C are given in Table 1. The critical weight of maturation of females (function f8) also decreases with temperature. We assume a sex ratio of 0.5. If we consider 67 eggs per female at 15°C (a temperature found in the North Sea in August) (Runge 1985) to be an optimum egg-laying rate and 0.3 μg C to be the egg weight (Carlotti et al. 1993), the maximum amount of carbon invested daily for reproduction is 20 μg C per female or ~20% of the female weight. This value lies in the range of estimates given by Corner et al. (1967). Due to a characteristic of the function relating reproduction to weight (*see* Carlotti and Nival 1992), the parameter P10 is equal to twice the amount of carbon invested daily in reproduction, in this case 40 μg C ind^{-1} d^{-1}. Carlotti and Nival (1992, their figure 5) explained how this function, f8, changes with temperature. Determining hatching and molting times of N1 and N2 is done with the formula of Corkett et al. (1986). Molting rate of other stages is related to growth rate and weight, according to an assumption explained in detail by Carlotti and Nival (1992). Individuals that reach these critical values molt immediately, which explains the high values of P17.

Few estimates of mortality in natural populations of *Calanus* copepods have been published, and such values most often pertain to whole populations or to naupliar and copepodite stages. In our model, we set a basic constant minimum mortality, which takes into account both predation and natural mortality, at 4% for nauplii and 2% for copepodite and adult stages. A complementary minimum mortality was added for N6, which is a critical stage in the life of copepods. Natural mortality is due to food shortage, temperature extremes, and old age within each stage. These causes are simulated by our model, which uses a hyperbolic relationship between growth rate and mortality rate (*see* Carlotti and Nival 1992). Maximum mortality rates are 10% for the feeding naupliar stages and early copepodites (Mullin and Brooks 1970*b*) and 5% for C5 and adults. Eggs, N1, and N2 have a constant mortality of 5%. These values were estimated from the stage abundances of *C. finmarchicus* during FLEX'76 (Bossicart ICES CM1980/C3).

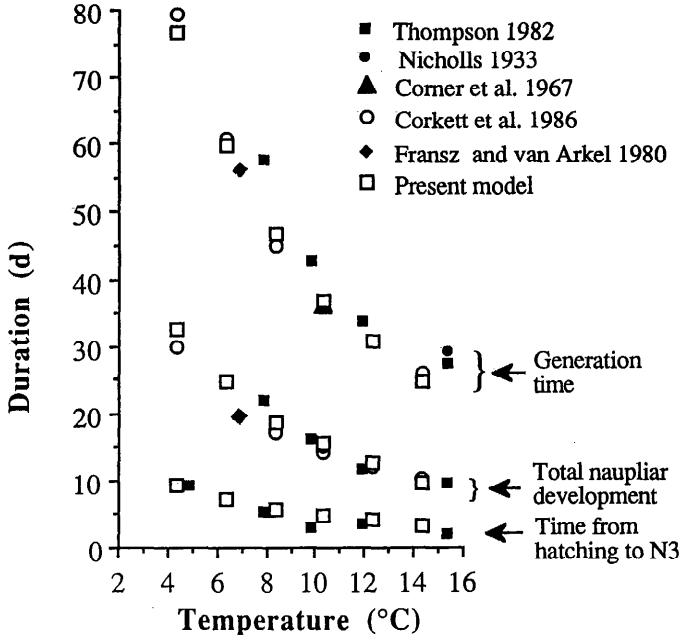

Fig. 2. Plot for *Calanus finmarchicus* showing simulated and published durations of its nonfeeding period and naupliar and total development times for different temperatures and nonlimiting food conditions.

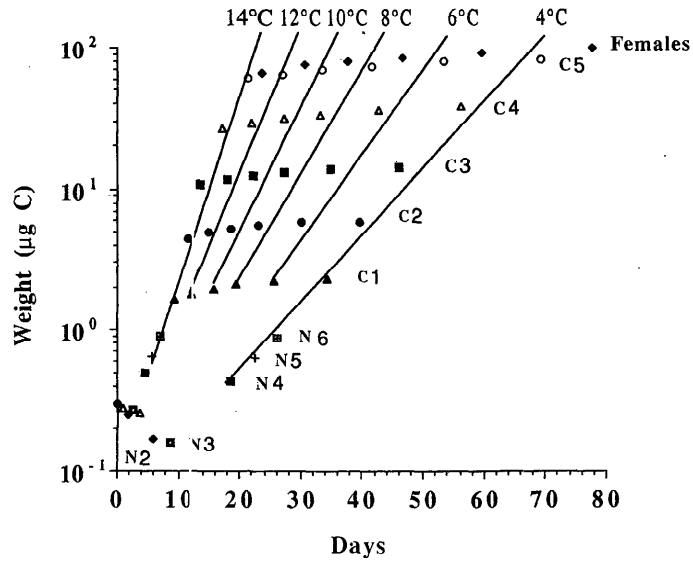

Fig. 3. Plot for *Calanus finmarchicus* showing simulated temporal development of stage weights at different temperatures and with nonlimiting food in a semilogarithmic scale. The weights are noted at the moment of maximum abundances during the first generation. Lines are exponential adjustments of copepodite weights.

Zooplankton model dynamics under laboratory conditions—In our model, the durations of the stages and growth curves are not parameters of the model but simulation results. These results follow the growth rate, which depends on metabolic rates that are controlled by environmental factors. In Figs. 2 and 3, we compare these outputs with published results from cultures grown under stable food and temperature conditions. Corkett et al. (1986) showed that the stage durations follow hyperbolic functions of temperature, which our findings mirror. The Q_{10} calculated between 4 and 14°C for the times of development from spawning to N3, C1, and adult are 3.64, 3.70, and 3.20. Mullin and Brooks (1970*a*) obtained a Q_{10} of 3.67 for the complete development of *C. helgolandicus*.

Growth does not seem to be exactly exponential from N3 to C5, which means that the specific growth rate is not constant for all developmental stages. Obviously, the rate is higher for C1 to C3 than for C4 to females. The nonfeeding period before N3 and the time-dependent molting to N2 and to N3 induces a decrease in weight. The first feeding stage, N3, must recover from these losses and reach critical weight before molting into N4, which makes the N3 stage longer. Average growth rates (during the whole life from egg to adult) range from 0.08 d^{-1} at 4°C to 0.24 d^{-1} at 14°C, which implies a Q_{10} for growth of 3.0. If we estimate growth rate from exponential adjustments of copepodite weights, we obtain 0.09 d^{-1} at 4°C and 0.36 d^{-1} at 14°C. These results are consistent with those obtained for closely related *Calanus* species (Vidal 1980). The modeled egg production process, which does not account for metabolism of reserves and egg formation, is probably too simple, whereas maximum egg production under optimum food conditions and for temperatures ranging from 6 to 14°C follows the rates given by Runge (1985, his figure 2).

Assumptions of the coupled model for the North Sea—We need to make assumptions concerning the vertical distribution and biology of the *C. finmarchicus* population. We propose that after ascent of the overwintering stages of the population to the North Sea shelf, the population in the central North Sea remains local. We assume that C5 and adult stages present at the end of winter become active when the temperature is >4.5°C and the food concentration is >0.04 g C m^{-3}. In fall, when temperature and phytoplankton decline to these same values, the surviving individuals return to the overwintering state, and their metabolism stops.

Initial overwintering weights of C5 and females were considered high values in the simulations, and weights above the critical weight of females were transformed into eggs in spring. We adopted a homogeneous distribution of zooplankton in the upper layer of 30-m depth for all stages. During winter months, we put inactive individuals in the same upper layer for model simplicity.

We assume that the available food concentration F for all the stages of the population is the mean value of the food concentration (phytoplankton and eventually other resources) in the layer occupied by zooplankton. We assume that copepods feed continuously if there is food present. Phytoplankton grazing GRAP(z, t) is proportional to phytoplankton concentration P(z, t) and is cal-

Table 2. Processes coupling the zooplankton submodel to the other components: $N_{i,j}$—abundance; $W_{i,j}$—weight; $I_{i,j}$—ingestion; $EG_{i,j}$—egestion; $EX_{i,j}$—excretion; $M_{i,j}$—mortality for individuals in age class j of stage i. Of the 13 stages from egg to adult, the number of age classes, $NC_{(i)}$, varies with stage; $P_{(z,t)}$—phytoplankton concentration; g_p—P:C ratio; p_M—percentage of remineralized dead phytoplankton in the water column; p_F—percentage of remineralized fecal material in the water column; p_Z—percentage of remineralized dead zooplankton in the water column; z_{max}—upper reach of zooplankton distribution; z_{min}—lower reach of zooplankton distribution.

	Averaging of temperature and food in the upper layer	
T	Mean temperature	$T(t) = \frac{1}{z_{max} - z_{min}} \int_{z_{min}}^{z_{max}} T(z,t)$
F	Mean food available for zooplankton	$F(t) = \frac{1}{z_{max} - z_{min}} \int_{z_{min}}^{z_{max}} P(z,t)$
	Outputs of the zooplankton submodel	
GRAZ	Grazed material	$GRAZ = \sum_{i=1}^{13} \sum_{j=1}^{NC(i)} I_{i,j}N_{i,j}$
FECP	Total fecal pellet material	$FECP = \sum_{i=1}^{13} \sum_{j=1}^{NC(i)} EG_{i,j}N_{i,j}$
MORZ	Total cadaverous material	$MORZ = \sum_{i=1}^{13} \sum_{j=1}^{NC(i)} M_{i,j}N_{i,j}W_{i,j}$
EXCR	Excretion of dissolved metabolic products	$EXCR = \sum_{i=1}^{13} \sum_{j=1}^{NC(i)} EX_{i,j}N_{i,j}$
	Repartition of zooplanktonic effects on the water column, $z_{min} \leq z \leq z_{max}$	
GRAP	Copepod grazing	$GRAP = GRAZ\frac{P(z,t)}{F(t)}$
REMI	Total remineralization	$REMI = g_p(REMP + REMF + REMZ)$
REMP	Remineralization of dead phytoplankton	$REMP = p_M MORP$
REMF	Remineralization of fecal pellets	$REMF = p_F FECP$
REMZ	Remineralization of zooplankton cadavers	$REMZ = p_Z MORZ$
	Formation of benthic detritus	
SEDI	Losses of particulate material from water column	$SEDI = (1 - p_M)MORP + (1 - p_F)FECP + (1 - p_Z)MORZ$

culated for each depth (Table 2). The products of zooplankton metabolism, which enter the model's nutrient compartment (i.e. excretion, remineralized fecal pellets, and dead bodies), are evenly distributed throughout the upper layer. The remaining fecal pellets and dead bodies fall immediately to the benthic detritus compartment.

Density-dependent predation is not represented in our simulation, although our model can easily integrate this phenomen; however, we included a constant minimum mortality in all simulations.

North Sea simulations—The coupled model was used to show the importance of differential dynamics of stages as related to the environment. First, runs were performed with the annual plankton dynamics in the central North Sea at the position of the ocean weather ship (OWS) *Famita* (57°N, 3°E), and the results were compared with those of Radach and Moll (1993) for 1984 (*see* their figure 23). The goal was to see how the population is driven by physical forcing. Second, we simulated the spring plankton dynamics in the northern North Sea at the position of the Fladen Ground Experiment (58°55'N, 0°32'E) in spring 1976 (*see* Radach et al. 1984) with the same model. The goal here was to study the link between phytoplankton and development of the zooplankton population. Because detritus production in this area is important during this period, we introduced pelagic detritus in our model to attempt to reproduce the observations made during FLEX'76.

Equations and numerical scheme—For the biological part of the model, the system of equations consists of two

Table 3. Differential equations for pelagic detritus and new processes. Detritus concentration PD(z,t); turbulent diffusion coefficient—A_v; phytoplankton sinking velocity w_S; detritus sinking velocity—w_D; detritus remineralization rate—r_D; height of water column—H. Other abbreviations as in Table 2.

PD	$\frac{\partial PD(z,t)}{\partial t} = DIFD - SIND + MORD + FEPD + MOZD - GRAD - REMD$	
POC	$\frac{\partial POC(z,t)}{\partial t} = \frac{\partial P(z,t)}{\partial t} + \frac{\partial PD(z,t)}{\partial t}$	
POC	Particulate organic C	$POC(z,t) = P(z,t) + PD(z,t)$
F	Mean food available for zooplankton	$F(t) = \frac{1}{z_{max} - z_{min}} \int_{z_{min}}^{z_{max}} POC(z,t)$

Zooplankton and phytoplankton equations given in Table 2

Pelagic detritus equation

DIFD	Turbulent diffusion of pelagic detritus	$DIFD = \frac{\partial}{\partial z}\left(A_v \frac{\partial P}{\partial z}\right)$
SIND	Sinking of pelagic detritus	$SIND = w_D\left(\frac{\partial PD}{\partial z}\right)$
MORD	Flux of dead phytoplankton	$MORD = p_M MORP$
FEPD	Flux of fecal pellets	$FEPD = p_F FECP$
MOZD	Flux of zooplankton carcasses	$MOZD = p_Z MORZ$
GRAD	Copepod grazing on pelagic detritus	$GRAD = GRAZ \frac{PD(z,t)}{F(t)}$
REMPD	Remineralization of pelagic detritus	$REMPD = r_D PD$

Nutrient equation

REMI	Total remineralization	$REMI = REMPD$

Benthic detritus equation

$F_P(z)$	Flux condition at the boundary for phytoplankton and detritus	$F_P(II) = -w_S P(z,t)_H - w_D PD(z,t)_H$

nonlinearly coupled second-order partial differential equations that simulate changes in the local concentrations of phytoplankton and phosphate, two ordinary first-order equations for light (Beer's equation) and benthic detritus (Radach and Moll 1993, part 2), and a subsystem of 26 ordinary and nonlinear first-order differential equations for zooplanktonic stage dynamics and growth (Carlotti and Sciandra 1989, their table 2). The processes linking the zooplankton submodel to Radach and Moll's (1993) model are presented in detail in Table 2. The values of the parameters for the copepod submodel are explained above. Other parameters adopt the values given by Radach and Moll (1993, their table 1) for their annual simulation. When we simulated the spring dynamics at the FLEX'76 station, we changed only the depth (150 m) and the C : Chl ratio, which was calculated to be 15 during FLEX'76 (Radach et al. ICES CM1980/C3). For the FLEX'76 simulations, the additional equations and processes relating to the model's pelagic detritus compartment are presented in Table 3.

The equations for light, phytoplankton, phosphate, and detritus are solved numerically by a combination of explicit difference schemes (*see* Radach and Moll 1993) with a time step of 75 s, and the zooplankton subsystem is solved by fourth-order Runge-Kutta numerical integration with a time step of 3 h. The runs were performed on a Siemens computer (7890F) with the MSF system. For a yearly simulation, one run lasted 8 min. For the FLEX'76 simulations, the copepod submodel was called at each integration step of the main model (every 75 s), with one run lasting 30 min.

Results

Annual plankton cycle—Radach and Moll (1993, figure 23) presented concepts, results, and validations of the physical and biological parts of the model with zooplankton forcing and gave the annual physical and biological dynamics at the OWS *Famita* site for 1984. For the same year, we present the simulation made with a dynamic population of *C. finmarchicus*. The simulated upper-layer temperature (Fig. 4A,B) began to increase at the end of March and reached 13°C at the end of August. A strong summer storm at the end of June broke up the thermocline and supplied the upper layer with nutrients. The thermocline formed again in July and progressively eroded in fall. The spring increase of temperature and the

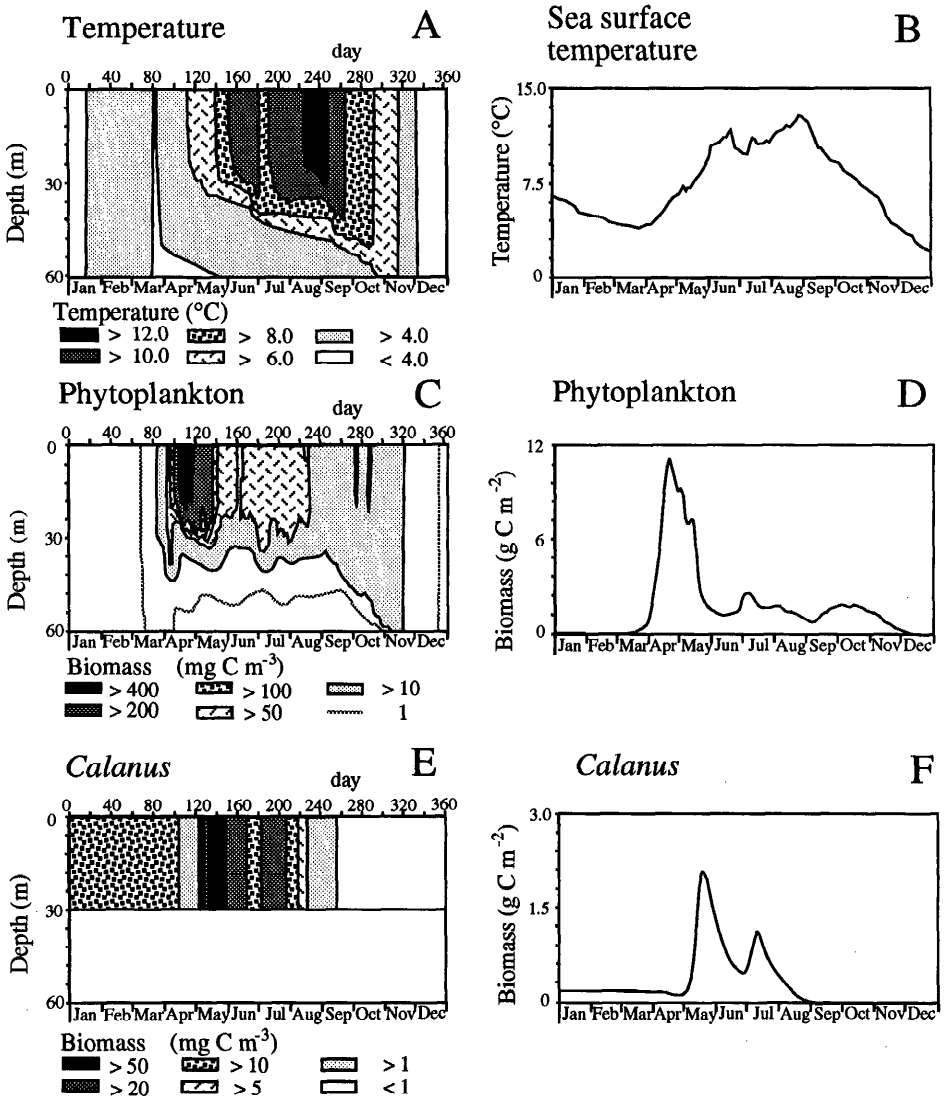

Fig. 4. Annual standard simulation. Shown are simulated profiles of temperature and evolution of upper-layer temperature and simulated profiles and integrated biomass of phytoplankton standing stock and of *Calanus finmarchicus* in 1984 for the OWS *Famita* site in the central North Sea. Initial densities of *C. finmarchicus* stages are 900 C5 m^{-2} and 450 females m^{-2}.

subsequent water-column stability induced the development of a phytoplankton bloom, which was followed by an increase in zooplankton (Fig. 4C–F). Food for *C. finmarchicus* copepodites, in the form of phytoplankton concentrations >50 mg C^{-3} (Fransz et al. 1991*a*), was found in the upper 30 m from April to mid-August. We assumed an even distribution of copepods in the upper 30 m. The initial overwintering stocks were composed of 30 C5 and 15 adult females m^{-3}, which resulted in an integrated biomass of 0.175 g C m^{-2}. This value was within the range of observed biomasses of C5 and females at the end of winter in the North Sea (Williams and Conway 1980). We did not study the dynamics of the overwintering population, which occurs in North Atlantic deep waters and arrives in the northern North Sea at the end of winter (Fransz et al. 1991*a*). The simulated biomass of *Calanus* in the surface layer from January to the beginning of April was artificial; for simplicity, we supposed the overwintering stock constant and inactive in the upper layer. When the copepods became active at the beginning of April, their biomasses began to decrease (Fig. 4E,F) because of a weight decrease of individuals subject to food limitation. The biomass then increased exponentially in the beginning of May, 4 weeks after the increase of phytoplankton (Fig. 4C,D). *Calanus* biomass and abundances decreased in the second part of May, when phytoplankton biomass decreased.

During summer, each meteorological event breaking the thermocline influences planktonic distributions and populations. The storm at the end of June eliminated the

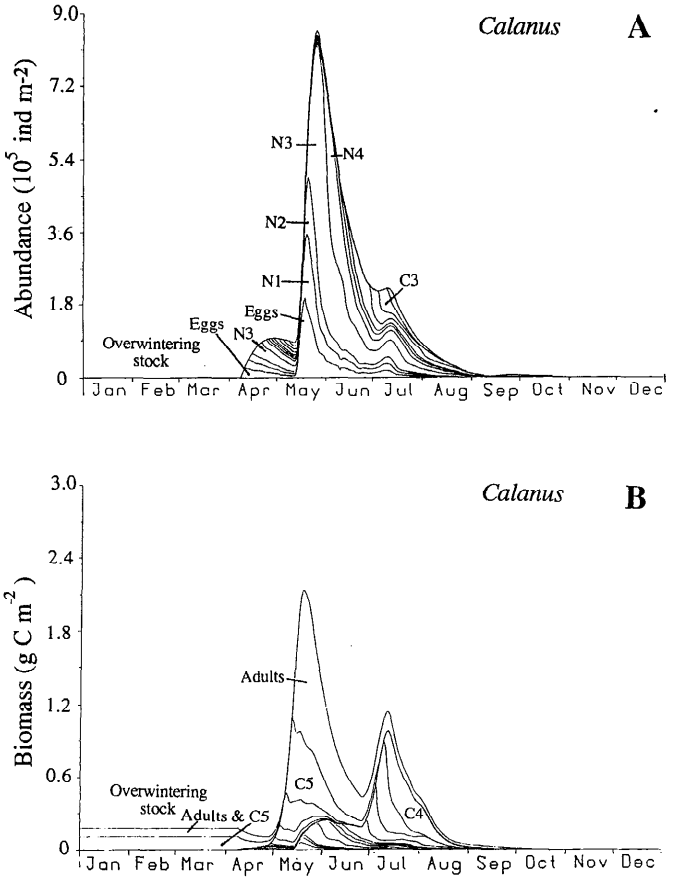

Fig. 5. Annual standard simulation. Shown are depth-integrated and cumulative abundances and biomasses of the stages of *Calanus finmarchicus*. Simulation begins with an overwintering stock of 900 C5 m^{-2} and 450 females m^{-2}.

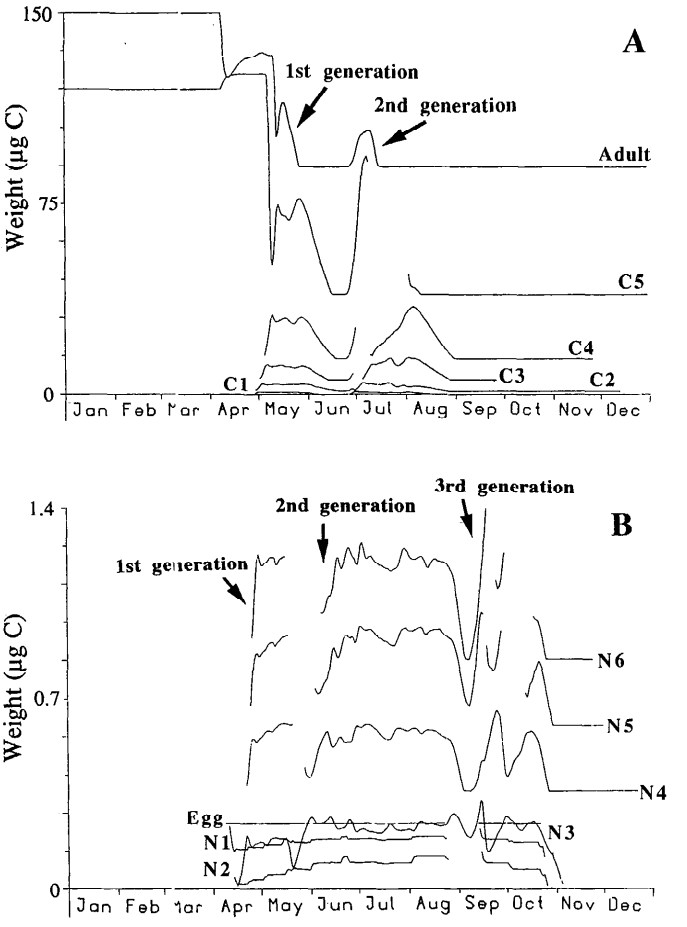

Fig. 6. Annual standard simulation. Shown are simulated mean body weights for copepodite and adult stages and for eggs and the six naupliar stages. Curves end when the abundance of individuals of each stage is <1% of the total population for naupliar stages and <0.5% for copepodite and adult stages.

thermocline (Fig. 4A), permitting an input of benthic regenerated nutrients, followed by a new development of phytoplankton and zooplankton (Fig. 4C–F). In fall, the concentrations of phytoplankton stayed low due to mixing of the entire water column. Because *Calanus* is unable to catch enough food when phytoplankton concentrations are low, there is no population increase in fall. We did not model the sinking of the population in deep waters, so the population starves in the upper layer and disappears.

The copepod population model simultaneously provides the time variations for numbers of individuals (Fig. 5A) and for biomasses of each stage (Fig. 5B). Initial concentrations of C5 and adult females were negligible in numbers, but not in biomass. Two complete distinct generations developed throughout the year, one beginning in April and the other in May. The peak of biomass in May was mainly due to the high proportion of C5 and adults of the first generation. Figure 5B clearly illustrates the overlap between the first and second generations. The second generation, present from the first spawning in May to the adults in August, seemed to develop slowly and had a high mortality rate (Fig. 5A). The phytoplankton peak in July permitted a new growth period for the second-generation copepodite stages, and some females produced a relatively small number of eggs to give a third generation in September (visible mainly in the growth curves).

Overwintering C5 and adults had stable weights from January to the beginning of April. In our model, copepod metabolism is not activated at such low temperatures and phytoplankton concentrations (Fig. 6A). We chose high winter weights for C5 and adults to represent reserves used for egg production. In April, the individuals became active and at first lost weight due to insufficient phytoplankton concentrations; thereafter, they grew by feeding on the phytoplankton bloom, and the adult females produced eggs. One hypothesis of our model was that egg weight (Fig. 6B) stayed constant, but weights within stages varied in several ways.

It is important to discriminate between the two phenomena that influence the evolution of mean weight in a stage: one phenomenon concerns the inflow and outflow of individuals passing through the stage, and the other

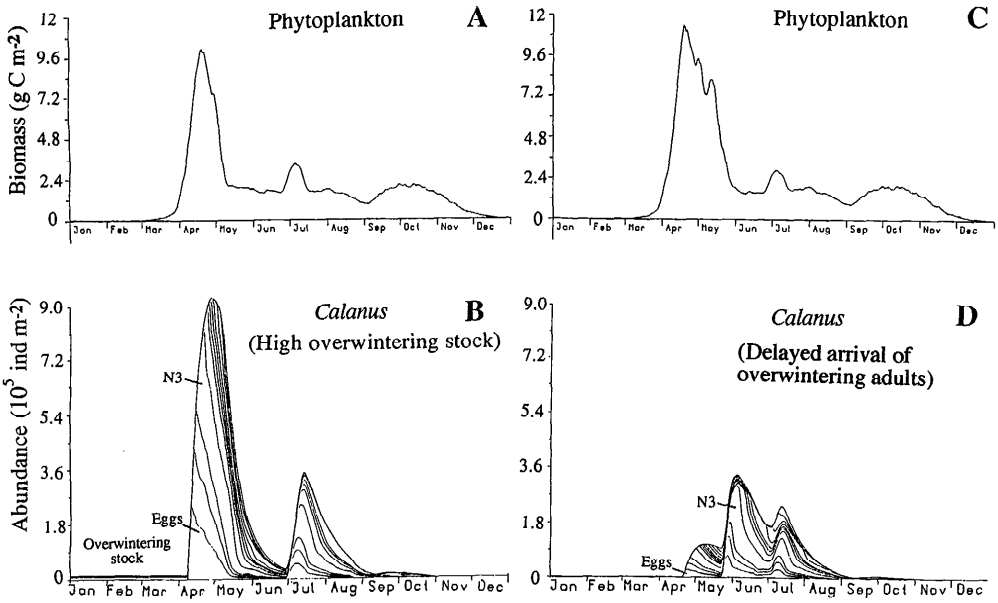

Fig. 7. Annual simulation. Shown are the effects of a high overwintering stock (A, B) and of a delayed ascent of overwintering individuals (C, D) for the depth-integrated biomass of phytoplankton and depth-integrated and cumulative stage abundances of *Calanus finmarchicus*. The simulation with a high overwintering stock begins with 9,000 C5 m^{-2} and 4,500 females m^{-2}; the simulated delay begins with the same densities as in Fig. 5.

phenomenon refers to the growth of individuals within the stage. Newly hatched individuals did not feed before stage N3 and thus lost weight during N1 and N2. The individuals of the first cohort, produced by overwintering individuals, grew rapidly; the eggs spawned in April became adults 30 d later. The second cohort mostly started in May and spread until the beginning of August; some precocious individuals reached the adult stage as soon as the end of June. By combining this information on growth with the dynamics of individuals, we can affirm that most individuals had a lower growth rate during the naupliar and copepodite phases with a low phytoplankton concentration in June; subsequently, the copepodite stages resumed exponential growth with the rise of phytoplankton in July. Individuals of a third cohort were produced in July by the precocious females of the second generation, and their development was concomitant with individuals of the second cohort. There were some individuals of a fourth cohort in September, but they developed no farther than stage N6 because of the lack of food and the severe decrease in temperature. Growth curves stopped because of the death of individuals, except for C5 and adults who entered overwintering status.

We investigated the effect of the initial overwintering stock on dynamics by starting with initial densities of 900 C5 and 450 adult females m^{-3}—10 times higher than in the basic simulation. These high initial copepod biomasses and densities changed the plankton dynamics in spring (Fig. 7A,B). Although this overwintering stock remained negligible in terms of total individuals, it was considerably higher in terms of biomass, with a value of 1.755 g C m^{-2}. During the exponential increase of phytoplankton biomass, zooplankton stock fell to 1 g C m^{-2}, then increased to 3 g C m^{-2} until 10 May, thus producing the same biomass as the basic simulation. Egg production lasted longer than 1 month (from the beginning of April to mid-May; Fig. 7B), with a first peak due to the initial females and a second very wide peak originating from the initial C5. The growth of the early individuals of the first cohort was fast during the naupliar stages, then slowed in stages C2 and C3 during mid-April because the resources needed to complete their development had been considerably reduced (Fig. 7A). Most of the individuals born later stopped their growth in the previous stages, which led to high biomasses in C2 and C3 when the biomass peaked in May. Phytoplankton biomass stayed between 1 and 2 g C m^{-2} in May and June, and lower competition for food among the living copepods permitted the survivors to resume their growth. The females spawned again after 15 May and produced a first cohort of second-generation individuals in May–June, whereas individuals whose growth had stopped in a naupliar stage reached the adult stage at the end of June and initiated a second cohort of the second generation in July.

The timing of the spring ascent of overwintering individuals also influences subsequent plankton dynamics (Fig. 7C,D). A 5-d delay in April for the *Calanus* ascent did not greatly affect the number of individuals in the first generation when compared with the basic simulation (*see Fig. 5*), but the delay did shift the appearance of females in the first generation. These females matured after the end of the bloom, and recruitment of the second generation was considerably reduced. At the beginning of July, the increase in phytoplankton permitted new egg

production; in addition, all stages resumed growth, which had been food limited during the last weeks of June.

Plankton bloom dynamics in spring—To understand in detail the dynamics of the pelagic ecosystem during the crucial spring period, we simulated the dynamics of the ecosystem from 5 April to 6 June 1976 and compared them to the data obtained during FLEX'76. The physical model was slightly adapted to the Fladen Ground area, thus the bottom is 150 m deep. The main features of the spring plankton bloom in the northern North Sea in 1976 that we wanted to simulate are presented by Radach (1980, his figure 1), Radach et al. (1984, their figure 1), and Krause and Radach (1989, their figure 2).

In our model runs, the initial concentration of phytoplankton was set at 0.3 mg C m^{-3} at the surface and reduced by 1.66% m^{-1} at a depth of 60 m (Gassman and Gillbricht 1982). We assumed that a population of *C. finmarchicus* arrived in the FLEX'76 area on 22 April via currents (*see* figure 1 of Radach 1983), but remained isolated afterward. The initial population had no eggs and no nauplii N1–N5, 1,000 N6, 400 C1, 70 C2, 70 C3, 70 C4, 80 C5, and 140 adults m^{-3} (Krause and Trahms 1983), for a total biomass of 0.0356 g C m^{-3}.

The first simulations, which took into account only the dynamics of the phytoplankton and zooplankton, did not reproduce the observations from FLEX'76 (Krause and Trahms 1983). The phytoplankton bloom was large and *Calanus* quickly grazed it down, but the copepodite stage abundances obtained in the simulation were <20% of the numbers observed in May. Complementary simulations with higher initial numbers of individuals did not change the results; the high initial *Calanus* biomass quickly grazed all the phytoplankton, resulting in a low phytoplankton standing stock in May and a high mortality of zooplankton. This result was similar to results obtained in the yearly simulations. We inferred that the development of the observed *C. finmarchicus* population was possible only if there were a complementary source of nutrition, either detrital remains or microzooplankton. Therefore, we added a pool of pelagic detritus to our model because Gassmann and Gillbricht (1982) had measured high levels of pelagical detritus in the upper 30 m during FLEX'76 (their figure 1). All the processes that enriched the benthic pool of detritus in the previous model (Fig. 1, i.e. phytoplankton mortality, zooplankton excretion, fecal pellet production, and death of copepods) supplied a pool of detritus to the water column. This material sank at a rate of 2 m d^{-1} in this new version of the model. The new processes are described in Table 3.

The simulated temperature profiles during the FLEX'76 period exhibited stratification in May and June (Fig. 8A). Temperatures progressively increased in the upper layer from 6°C on 5 April to 9.5°C in June.

The phytoplankton bloom in the simulation took place between the end of April and 10 May (Fig. 8D). Detritus (Fig. 8C) was abundant mainly when the phytoplankton concentration exceeded 200 mg C m^{-3}, and its maximum concentration was deeper than the 30-m layer. The *C. finmarchicus* biomass (Fig. 8E) increased after 8 May and was maximal between 28 May and 5 June, with a value in the range of the FLEX'76 observations. The profiles of phytoplankton and zooplankton show an apparent gap in the food supply for zooplankton; this gap may be filled by detritus, as indicated by the POC concentration (Fig. 8D).

At the end of the simulation, when the zooplankton biomass became high in the upper 30 m, phytoplankton biomass was found primarily in deeper parts of the upper layer. Strong grazing pressure eliminated phytoplankton cells in the shallow part of the upper layer and diminished self-shading. In our simulation, the copepods do not migrate. Therefore, phytoplankton and detritus were not grazed below the thermocline and provided a high level of POC after 20 May below 30-m depth. The abundances of copepodite stages in the water column (Fig. 9) are consistent with observations by Krause and Trahms (1983), but the simulated numbers for the nauplii are twice as high as their observations. Females present on 22 April produced the first peak of eggs. The development of these individuals can be followed through stage C5, but they do not reach adult stage before the end of the simulated period. The adult females, who had been the initial individuals in stages N6–C5, spawned eggs continuously during a month-long period after 27 April. These eggs furnished the high densities of individuals in stages C1–C5 at the end of the FLEX'76 period and were of the same magnitude as densities observed by Krause and Radach (1980). The last peak of eggs was produced by females from the development of the initial N6 cohort.

Growth curves (Fig. 10) clarify this interpretation of the dynamics. When the population arrived in the area, only the N6 nauplii grew because they could feed on lower concentrations than could the other copepodite stages. By contrast, the initial copepodite stages lost weight during the first days of the bloom, then grew normally. From 22 April to 19 May, the mean weight of females fluctuated slowly because of continuing egg production. The copepodite growth curves fluctuated because there were successive cohorts produced by females from initial densities in different stages. Weight of initial females decreased as they produced eggs. The eggs spawned by these females generated a distinctive cohort, with rapid naupliar growth from 24 April to 9 May (Fig. 10B) followed by a slow growth in the copepodite phase from 9 May to the beginning of June (Fig. 10A). The cohort produced by the initial group of N6 nauplii developed through the copepodite stages from 29 April to 25 May. These individuals became adults after 25 May and produced the last peak of eggs seen in Fig. 9.

Discussion

Comparison of simulation and FLEX'76 data—The simulation of the thermal stratification of the water column during FLEX'76 shows an increase in the upper-layer temperature (Fig. 8A) and is consistent with the observations of Soetje and Huber (*see* figure 2 of Krause and Radach 1989).

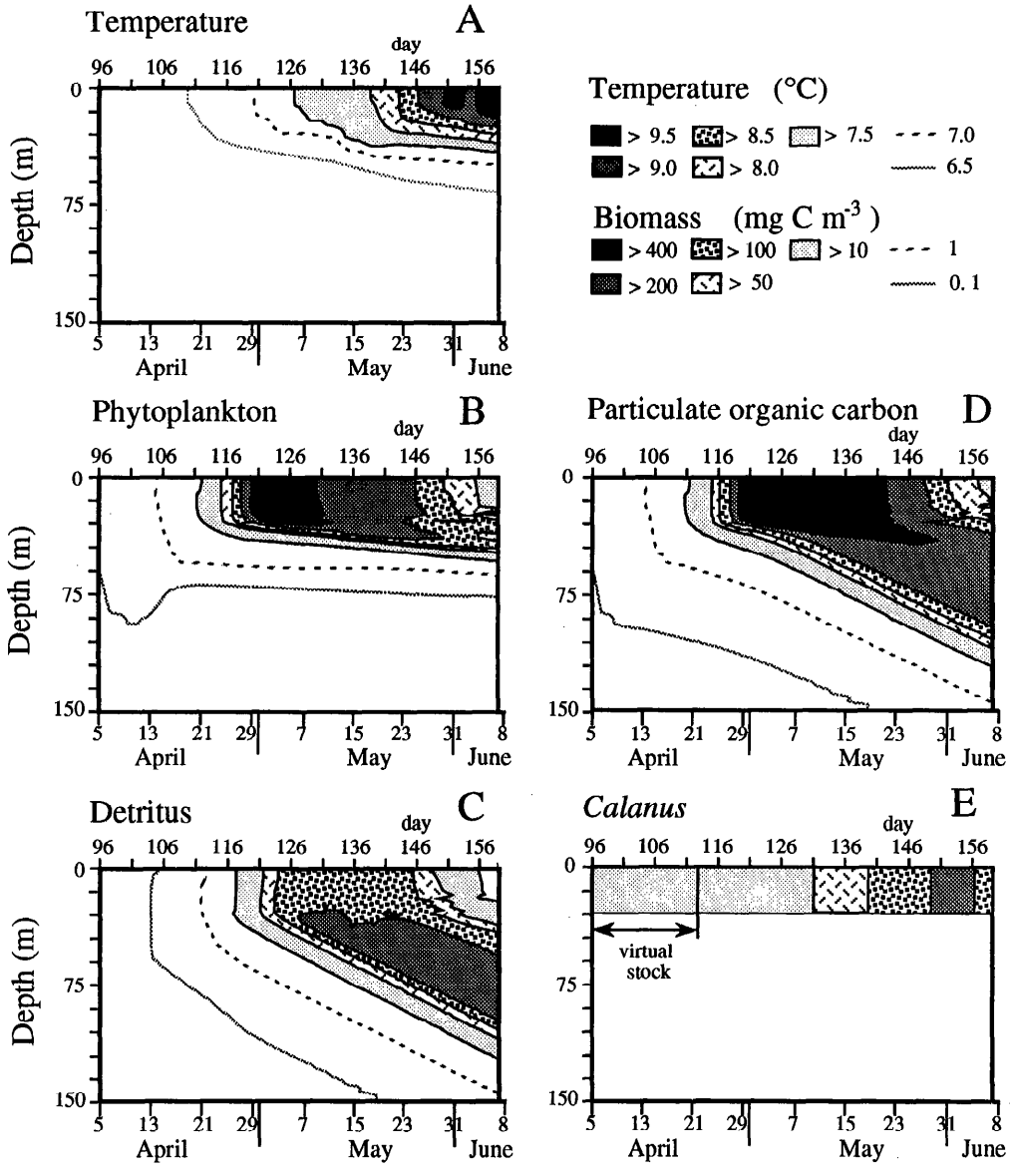

Fig. 8. Standard FLEX'76 simulation. Shown are simulated profiles of temperature, phytoplankton, pelagic detritus, particulate organic C, and *Calanus finmarchicus* during FLEX'76. The population of *Calanus* begins with the stage densities (per m²) observed by M. Krause (pers. comm.) on 22 April: 1,000 N6; 400 C1; 70 C2; 70 C3; 70 C4; 80 C5; and 140 adults.

The simulated biomass profiles for phytoplankton and detritus (Fig. 8B,C) can be compared with the observed distributions of active chlorophyll pigments and phaeophytin pigments, respectively (figures 2 and 4 of Radach et al. ICES CM1980/C3; figure 1 of Radach et al. 1984; figure 2 of Krause and Radach 1989). Our simulated phytoplankton biomass starts with an exponential growth that is coincident with the observed bloom of phytoplankton. The maximum concentrations of simulated phytoplankton are higher than those observed because our simulated grazing rate is too low for the first days of the bloom. We also note that the phytoplankton bloom lasts longer when we include pelagic detritus because of the lower grazing pressure on phytoplankton when *Calanus* has two available food sources; we assume that copepods feed equally on phytoplankton and detritus. In reality, copepods probably prefer fresh living phytoplankton when it is present; if it is unavailable, they switch to detritus. During FLEX'76, ingestion by zooplankton exceeded production of phytoplankton (Williams and Lindley 1980*a*; Daro 1980; Radach et al. 1984). Other mesozooplanktonic species (e.g. *Thysanoessa inermis, Oithona* sp.) also were observed before the spring bloom (Williams and Lindley 1980*a*; Krause and Trahms 1983) and may have acted as a fine but decisive control on the phytoplankton at the beginning of the bloom (Lindley

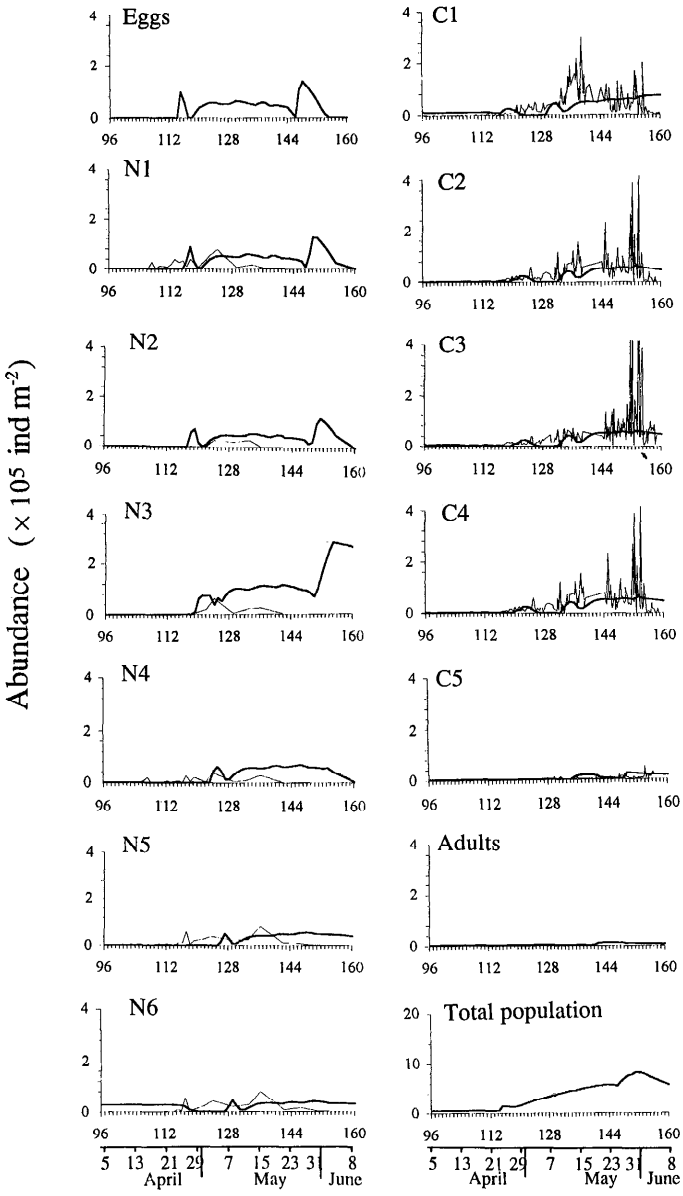

Fig. 9. Standard FLEX'76 simulation. Shown are simulated depth-integrated abundances of individuals of *Calanus finmarchicus* stages during FLEX'76 for the water column (thick lines). Data for the naupliar and copepodite stages (thin lines) are from Krause and Trahms (1983).

and Williams 1980). There was high microbial activity (Gieskes and Kraay 1980), and these organisms also could have grazed on the phytoplankton biomass. The sedimentation of detritus occurred mainly after 4 April in our simulation (Fig. 8C), which coincides with timing in reported observations (*see* figure 4 of Radach et al. ICES CM1980/C3). The abundant total POC in the upper layer from 28 April to 21 May in our simulation (Fig. 8D) is consistent with the findings reported by Gassmann and Gilbricht (1982, their figure 1), although POC concentration decreased as early as 10 May.

The approximation of a homogeneous distribution of *Calanus* in the upper 30 m (Fig. 8E) is essentially correct at the beginning of FLEX'76, but not after mid-May (*see* figure 5 of Krause and Radach 1989). The simulated development of *C. finmarchicus* nauplii and copepodites (Fig. 9) is chronologically similar to the observations of Krause and Trahms (1983), and the simulated abundances of copepodite and adult stages have the proper magnitude. However, our simulations suggest that the in situ naupliar densities must have been greater than those counted by Krause and Trahms (1983, their figure 4), based on the assumption of local population dynamics. The review by Fransz et al. (1991*a*) suggested that the population in the Fladen Ground is subject to advection and that there is an import of copepodites. Our model densities, beginning 22 April, simulate densities observed by Krause and Trahms (1983) at the end of May.

Both simulated growth and development suggest that no more than one generation could occur during the FLEX'76 study period and that growth of the population also could have been possible based on local food supply. Gamble (1978, his figure 2) presented the growth of the mean dry weight of the subgroup of C4, C5, and adults from 25 April to 10 May and noted an "inversion of stages" on 10 May marked by a decrease of this mean weight. Our simulation (Fig. 10) indicates that such an inversion probably was caused by the simultaneous presence of several cohorts.

The simulated *C. finmarchicus* biomasses (Fig. 11A), which are the combined individual growth and abundances, are comparable to those observed by Krause and Radach (1980). Daro (1980) studied *C. finmarchicus* grazing in the upper 40 m from the end of May to the beginning of June and calculated production from respiration data and egestion for the same period (*see* Daro 1980, table 3). Our simulated ingestion rate (Fig. 11C) is comparable to Daro's 23 May data, but our ingestion rate decreases in June, whereas Daro observed a maximum grazing of 2.5 g C m^{-2} d^{-1} during this time. Our simulated production of fecal pellets (Fig. 11E) is of the same order as the simulations and observations in June, but is overestimated by the simulations in May. Simulated excretion is lower than the estimated respiration losses (Fig. 11B). Daily loss of matter by death is also an important process in the biomass balance of the population (Fig. 11D). The simulated productivity at the beginning of May is equal to that estimated by Fransz and van Arkel (1980). During the last 10 d of May, the simulated productivity is higher than Daro's (1980) values. In June, however, the simulated productivity falls, whereas Daro calculated a net production of 360 mg C m^{-2} d^{-1}. Our decrease in the simulated net production is correlated with the decline of the growth rate of older copepodites (Fig. 10A) and the decrease in egg production (Fig. 9) because of unfavorable feeding conditions in the upper 30 m (Fig. 8D). Fransz (ICES CM1980/C3) also found that the growth rate of the largest copepodite stages was low at the end of FLEX'76 and that the C5 "hesitated to become adult."

The time-integrated rates for phytoplankton production, copepod grazing, fecal pellet production, and ma-

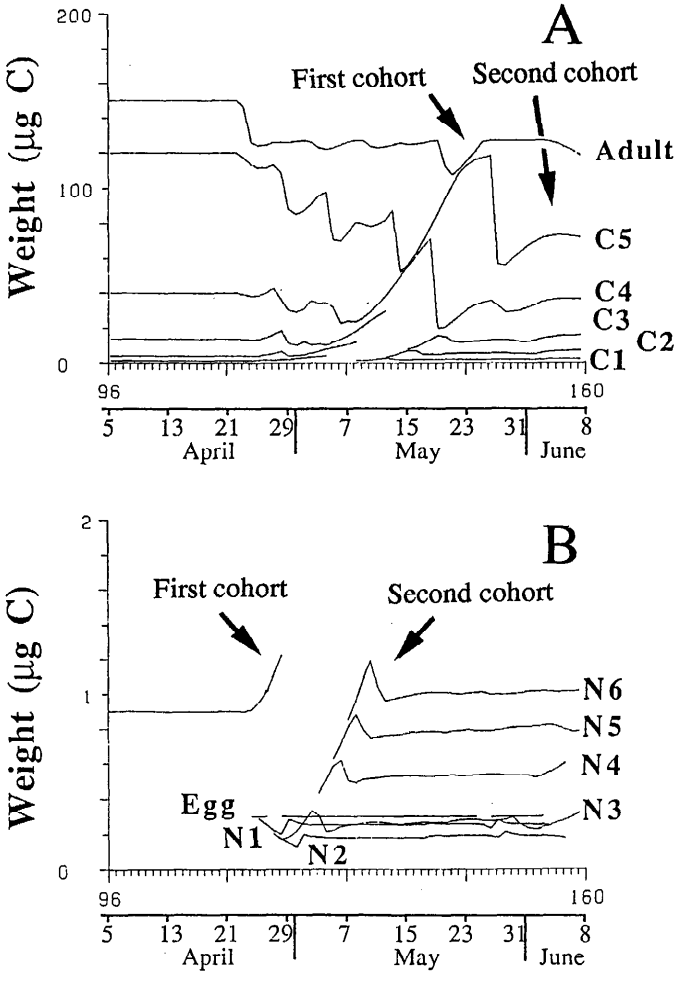

Fig. 10. Standard FLEX'76 simulation. Shown are simulated mean body weights for copepodite and adult stages and for eggs and naupliar stages.

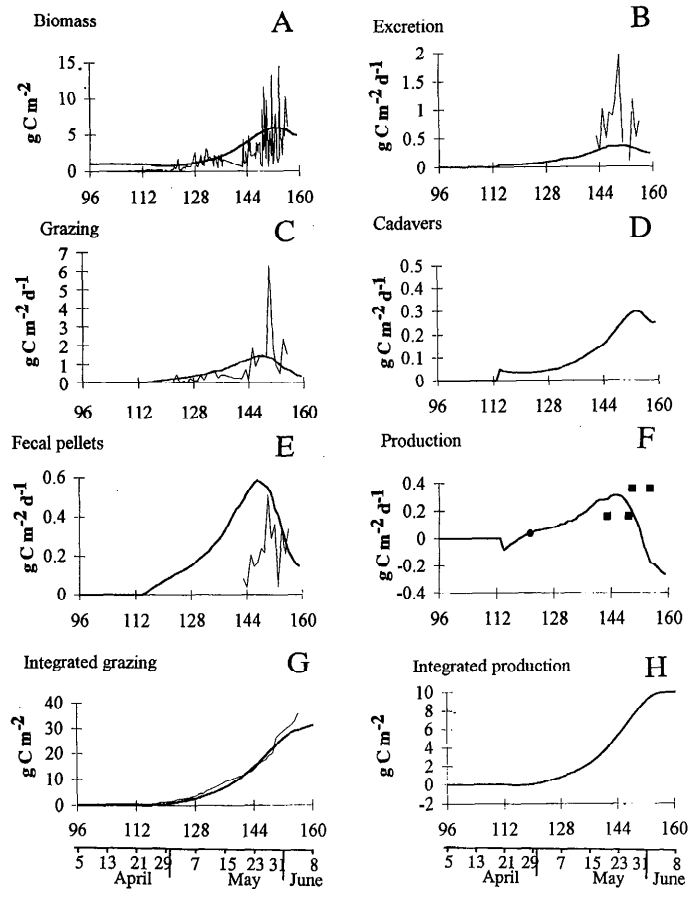

Fig. 11. Standard FLEX'76 simulation. Shown are simulated depth-integrated biomasses of *Calanus finmarchicus* (A) and the processes of excretion (B), grazing (C), production of dead bodies (D), and fecal pellets (E) (thick lines). Data (thin lines) are from Krause and Radach (1980) for biomass and from Daro (1980) for processes. Simulated production (F) of *C. finmarchicus* (line) is compared with the estimates of Fransz and van Arkel (1980) (●) and Daro (1980) (■). The simulated cumulative grazing (thick line) is compared with grazing calculated by Radach et al. (1984) (thin line) with the "POC limited approach" (G). Simulated secondary production (H) during the period of FLEX'76 is calculated as grazing minus fecal pellet production and excretion.

terial excreted by *Calanus* are also calculated by the model. For the FLEX'76 period, the simulated primary production reaches 49.4 g C m^{-2}, which is in the range of production estimated by several investigators (*see* Radach et al. 1984). The simulated integrated grazing (Fig. 11G) is significant after 16 May and reaches a cumulative value of 30.85 g C m^{-2} at the end of the simulation. Only 8.3 g C m^{-2} were grazed from phytoplankton, illustrating the importance of detritus. This grazing value is lower than all values estimated by Radach et al. (1984), except when they assumed the amount of grazing to be 10% of the biomass. The simulated secondary production of *C. finmarchicus* during FLEX'76 (Fig. 11H) reaches 10 g C m^{-2}.

Effect of diel migration at the end of FLEX'76—The simulated biomass of the entire population reaches a maximum before the end of the FLEX'76 period, there is then a net decrease, resulting in a stock of 5 g C m^{-2} at the end of FLEX'76. This decrease was not observed in reality (Krause and Radach 1980) but is caused by food-limited grazing after 27 May (Fig. 11C), which diminishes and stops growth of individuals (Fig. 10A). Krause and Radach (1989) showed that all the copepodites carried out diel vertical migrations after 15 May, but never before this date. The mean depth of the center of gravity of the copepodite and adult stages of *C. finmarchicus* was 21 m during the algal bloom; thus, the assumption of an even distribution of *C. finmarchicus* in the upper 30 m is largely correct for this period. After the algal bloom, the mean depth of the center of gravity was 34 m, and the copepods carried out diel vertical migrations.

We assumed that the entire *Calanus* population mi-

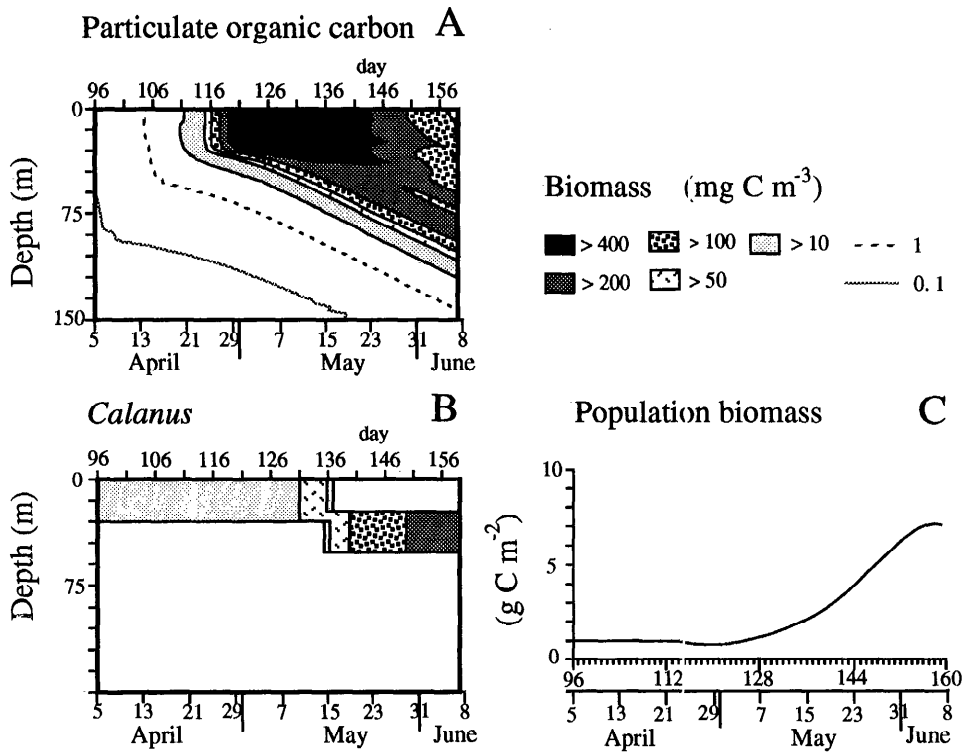

Fig. 12. Simulation during spring with migration. Shown are simulated profiles of particulate organic C and *Calanus finmarchicus* during the period of FLEX'76, and the integrated biomass of *C. finmarchicus*. The initial conditions (stage abundances and weights) are identical to those of the standard FLEX'76 simulation in Fig. 10. The migration is affected after 15 May from 0–30 m to 20–50 m. The figure shows only one position per day at noon, but the organisms actually migrate following a periodical sinusoidal function.

grated from 0–30 m at night to 20–50 m during the day (Fig. 12B). The biomass of *Calanus* then increased until the end of FLEX'76 (cf. Figs. 12C and 11A). The individuals could have fed in deeper regions (cf. Figs. 12A and 8D) and their growth continued. This result suggests that migration can give a metabolic advantage when the total food sinks to deeper layers. Daro (1980) noted the strongest diel vertical migrations when the available food became scarce.

Annual cycle of Calanus finmarchicus—Williams and Lindley (1980*b*) suggested that the success and strength of the overwintering population is fundamental to the strength of the developing spring cohorts. Comparing our annual simulations that begin with different overwintering copepod biomasses or with different dates of ascent of overwintering stages (Figs. 5, 7), it is obvious that initial conditions influence the dynamics of both phytoplankton and *Calanus* populations. Our simulations show that a too high initial biomass of overwintering zooplankton can have a negative effect on the resulting population.

At the beginning of the spring bloom, development of the first generation of *C. finmarchicus* lasts 1 month if it is initiated by a normal overwintering stock (Figs. 5, 7D). During this bloom period, the limiting growth factor is temperature, which increases slowly in the upper layers. Pedersen and Tande (1992) showed that in the Barents Sea the naupliar stages spawned by overwintering females have different optimum temperatures for their growth; these optimum temperatures are linked with the spring increase in temperature. Such a phenomenon also may play an important role in the North Sea, as well as in the timing of ontogenic vertical migration of overwintering individuals to the surface layers. The highest population biomass is produced by the last stages of the first generation, and the highest abundances occur with the first stages of the second generation, as observed during FLEX'76 (Krause and Trahms 1983; Krause and Radach 1980). The highest grazing pressure from *C. finmarchicus* comes from the last stages of the first generation, which reduces the phytoplankton stock in May. Therefore, the simulated bloom is limited by nutrients at the end of April, as in the simulation made by Radach and Moll (1993, their figure 23) with zooplankton forcing, and then by the grazing of late copepodites of the first generation. The success of the first generation produced by overwintering females of *Calanus* can play a role in bloom limitation (Fig. 7A,B).

In the North Sea, the peaks of phytoplankton are shorter (Radach et al. ICES CM1980/C3) than in our annual simulation. Obviously, grazing by *C. finmarchicus* that occurs mainly in May cannot be the only process limiting

the phytoplankton bloom. Other grazers may play an important role during the first weeks of the bloom and probably are replaced afterward by the first generation of *C. finmarchicus*. Fransz and Gieskes (1984) suggested that microzooplankton play a role both as grazers of phytoplankton and as a food source for zooplankton. When we added a pelagic detritus compartment to the FLEX'76 simulations, the simulated stage abundances and biomasses finally had the right magnitude. We may reasonably assume that there is a link between microbial activity and detritus, and that copepods feed not only on detritus, but also on microbial organisms. An additional improvement to the model would be to add a microzooplankton compartment.

The growth curves for each stage are essential to clearly understand the stage dynamics. Our basic simulation shows a weight decrease in overwintering stages before the spring bloom, as observed by Tande (1982). A comparison between the first and the second generations (Fig. 6) reveals that the first is limited by temperature, whereas the second is clearly limited by food in June and July. The growth curves of copepodite and adult stages show that individuals of the second generation at the end of June and the end of July are the last C5s and adults of the year. Several workers (*see* Fransz et al. 1991*a*) have suggested that copepodites and adults sink into deeper layers as early as July, constituting the next overwintering population. This interesting result shows that growth, development, and life strategy must be understood together in relation to the environment.

Our model also could be used to study regional differences. *C. finmarchicus* is not the dominant copepod species after July in the North Sea, but the model provides some interesting results. The storm at the end of June induced a diffusion of bottom-regenerated nutrients into the upper layer and decreased sea-surface temperature; after this storm, phytoplankton biomass was between 50 and 100 mg C m^{-3}, and zooplankton biomass was between 10 and 20 mg C m^{-3}. These ranges are the same as those estimated by Peterson et al. (1991) for the second part of August in the Skagerrak.

Comparison of simulations with and without zooplankton forcing (Fig. 4; figure 23 of Radach and Moll 1993) shows that forcing influences phytoplankton dynamics differently than it does zooplankton dynamics. With forcing, the phytoplankton peak is lower and narrower because of high zooplankton biomass estimated from CPR (continuous plankton recorder) data. Moreover, the small peak of phytoplankton following the storm of the end of June seems to be shifted toward mid-July and is very low due to strong grazing pressure from the high biomass of zooplankton. In the simulation of zooplankton dynamics, the biomass of *Calanus* decreases after the spring bloom, so that regenerated nutrients that go into the upper layer are utilized for phytoplankton production, which is not immediately grazed. This summer production permits copepodite stages of the second generation to resume growth (Figs. 5, 6). In fall, the phytoplankton standing stock is evenly distributed over the entire water column, and concentrations are <50 mg C m^{-3}. Copepodites cannot develop in such situations. This result suggests that the decay of *C. finmarchicus* in fall and its replacement by other species could be due to changes in the physical environment rather than competitive pressure from other species.

Note that the dynamics of the *Calanus* population changes considerably when we use a high overwintering stock of C5s and females (Fig. 7A,B), but the evolution of phytoplankton standing stock in summer and fall is similar (cf. Figs. 4D and 7A). In the standard annual simulation, total phytoplankton production is 146.92 g C m^{-2} yr^{-1} from April to October, of which 21.04 g C m^{-2} yr^{-1} is grazed. If we include the production of fecal pellets and excretion, we obtain production values of ~ 10 g C m^{-2} yr^{-1}, which is in the range of secondary production values presented by Fransz et al. (1991*a*) for the northern North Sea. During the whole year, 14.3% of the phytoplankton production is grazed by *C. finmarchicus*. These values are high compared to other estimates (Nielsen and Richardson 1989) because *C. finmarchicus* has no competitors for grazing phytoplankton in our model. From a different site, Aksnes and Magnesen (1983) estimated *C. finmarchicus* grazing to be between 25 and 90% of the primary production. Joiris et al. (1982) presented a carbon budget for the Belgian coastal zone (*see* their table 1). They obtained a primary production rate of 170 g C m^{-2} yr^{-1} and a zooplankton grazing rate of 80 g C m^{-2} yr^{-1}. Their biomasses of detritus and microheterotrophic activity also were high in the ecosystem off the Belgian coast.

Conclusion

Because we used a 1-D water-column process model, we were able to use a detailed biological approach of population dynamics coupled with physical and biological variations in the water column during the year. The links between individual behavior and population dynamics of the copepod model allowed us to form a relationship between physiological rates and the evolution of zooplankton biomass. In our model, the development of *C. finmarchicus* adjusts itself to the dynamics of its food supply.

The threshold of food concentration above which copepods can survive seems to be an essential parameter at the beginning of the bloom and at the end of summer when the thermocline deepens. Copepod abundance depends on physical processes in the water column and on biological processes, such as phytoplankton growth and sedimentation. Following the work of Mullin and Brooks (1976) and Fernandez (1979), we established a lower threshold for naupliar stages than for copepodite stages. This phenomenon could be important at the beginning of the bloom when food concentration increases.

Our model allows us to reproduce realistic time lags between the availability of a new resource and the following growth of the population. The simulations show that the zooplankton population clearly misses the phytoplankton bloom if it is brief. Two complete generations

of *C. finmarchicus* develop in spring and early summer, and the overwintering stock of the following winter must be mainly formed in summer from individuals of the second generation because the third generation probably does not reach the last stages in time. Different stage distributions in overwintering stocks may dramatically change the stage dynamics of *C. finmarchicus* during the year but do not necessarily produce higher zooplankton biomasses because of competition for food.

Our simulated phytoplankton bloom was about twice as long as is usually observed. We therefore conclude that *Calanus* cannot be the main factor limiting the phytoplankton bloom in the northern North Sea. The growth of the first generation of *C. finmarchicus* has a 4-week delay before it reaches the last stages, and increases its grazing rate. Despite the long phytoplankton bloom in the simulation, the females miss the bloom and produce an insufficient second generation. We conclude that food sources other than phytoplankton are necessary to sustain growth of the *Calanus* population over spring and summer. One or several other factors play an essential role between phytoplankton and *Calanus,* both as grazers of phytoplankton and as food for *C. finmarchicus.* Micrograzers, which feed on phytoplankton and detritus and also are eaten by copepods, probably assume this role (Nielsen and Richardson 1989; Ohman and Runge 1994).

Zooplankton have characteristic growth and development rates that are important in ecosystem dynamics and should be considered in ecosystem models. These characteristics cannot be represented by bulk models of zooplankton. Our model is a first step in understanding how the population dynamics of a dominant species interact with the environment.

References

AKSNES, D. L., AND T. MAGNESEN. 1983. Distribution, development, and production of *Calanus finmarchicus* (Gunnerus) in Lindåspollene, western Norway, 1979. Sarsia **68:** 195–208.

CARLOTTI, F., M. KRAUSE, AND G. RADACH. 1993. Growth and development of *Calanus finmarchicus* taking into account the effect of temperature. Limnol. Oceanogr. **38:** 1125–1134.

———, AND P. NIVAL. 1992. Model of growth and development of copepod: Study of molting and mortality related to physiological processes during the course of individual moult cycle. Mar. Ecol. Prog. Ser. **84:** 219–233.

———, AND A. SCIANDRA. 1989. Population dynamics model of *Euterpina acutifrons* (Copepoda, Harpacticoida) coupling individual growth and larval development. Mar. Ecol. Prog. Ser. **56:** 225–242.

CORKETT, C. J., I. A. MCLAREN, AND J. M. SÉVIGNY. 1986. The rearing of marine copepods *Calanus finmarchicus* (Gunnerus), *C. glacialis* (Jaschnov) and *C. hyperboreus* (Kroyer) with comment on the equiproportional rule (Copepoda). Syllogeus Natl. Mus. Can. **58:** 539–546.

CORNER, E. D. S., C. B. COWEY, AND S. M. MARSHALL. 1967. On the nutrition and metabolism of zooplankton. 5. Feeding efficiency of *Calanus finmarchicus.* J. Mar. Biol. Assoc. U.K. **47:** 259–270.

DARO, M. H. 1980. Field study of the diel feeding of a population of *Calanus finmarchicus* at the end of a phytoplankton bloom. "Meteor" Forsch. Ergeb. Ser. A **22:** 123–132.

FERNANDEZ, F. 1979. Nutrition studies in the nauplius larva of *Calanus pacificus* (Copepoda: Calanoida). Mar. Biol. **53:** 131–148.

FRANSZ, H. G., J. M. COLEBROOK, J. C. GAMBLE, AND M. KRAUSE. 1991*a*. The zooplankton of the North Sea. Neth. J. Sea Res. **28:** 1–52.

———, AND W. W. C. GIESKES. 1984. The unbalance of phytoplankton production and copepod production in the North Sea. Rapp. P.-V. Reun. Cons. Int. Explor. Mer **183:**218–225.

———, J. P. MOMMAERTS, AND G. RADACH. 1991*b*. Ecological modelling of the North Sea. Neth. J. Sea Res. **28:** 67–140.

———, AND W. G. VAN ARKEL. 1980. Zooplankton activity during and after the phytoplankton spring bloom at the central station in the FLEX box, northern North Sea, with a special reference to the calanoid copepod *Calanus finmarchicus* (Gunn.). "Meteor" Forsch. Ergeb. Ser. A **22:** 113–121.

GAMBLE, J. C. 1978. Copepod grazing during a declining spring phytoplankton bloom in the northern North Sea. Mar. Biol. **49:** 303–315.

GASSMANN, G., AND M. GILLBRICHT. 1982. Correlations between phytoplankton, organic detritus and carbon in North Sea waters during the Fladenground Experiment (FLEX '76). Helgol Wiss. Meeresunters. **35:** 253–262.

GIESKES, W. W. C., AND G. W. KRAAY. 1980. Primary production and phytoplankton pigment measurements in the northern North Sea during FLEX'76. "Meteor" Forsch. Ergeb. Ser. A **22:** 105–112.

JOIRIS, C., AND OTHERS. 1982. A budget of carbon cycling in the Belgian coastal zone: Relative roles of zooplankton, bacterioplankton and benthos in the utilization of primary production. Neth. J. Sea Res. **16:** 260–275.

KIØRBOE, T., AND T. G. NIELSEN. 1990. Effects of wind stress on vertical water column structure, phytoplankton growth, and productivity of planktonic copepods, p. 28–40. *In* M. Barnes and R. N. Gibson [eds.], Trophic relationships in the marine environment. Aberdeen Univ.

KRAUSE, M., AND G. RADACH. 1980. On the succession of developmental stages of herbivorous zooplankton in the northern North Sea during FLEX '76. 1. First statements about the main groups of the zooplankton community. "Meteor" Forsch. Ergeb. Ser. A **22:** 133–149.

———, AND ———. 1989. On the relations of vertical distribution, diurnal migration and nutritional state of herbivorous zooplankton in the northern North Sea during FLEX '76. Int. Rev. Gesamten Hydrobiol. **74:** 371–417.

———, AND J. TRAHMS. 1983. Zooplankton dynamics during FLEX '76, p. 632–661. *In* J. Sündermann and W. Lenz [eds.], North Sea dynamics. Springer.

LINDLEY, J. A., AND R. WILLIAMS. 1980. Plankton of the Fladen Ground during FLEX '76. 2. Population dynamics and production of *Thysanoessa inermis* (Crustacea: Euphausiacea). Mar. Biol. **57:** 79–86.

MARINE ZOOPLANKTON COLLOQUIUM 1. 1989. Future marine zooplankton research—a perspective. Mar. Ecol. Prog. Ser. **55:** 197–206.

MARSHALL, S. M., AND A. P. ORR. 1958. On the biology of *Calanus finmarchicus.* 10. Seasonal changes in oxygen consumption. J. Mar. Biol. Assoc. U.K. **30:** 527–547.

MULLIN, M. M., AND E. R. BROOKS. 1970*a*. Growth and metabolism of two planktonic marine copepods as influenced by temperature and two types of food, p. 74–95. *In* J. H. Steele [ed.], Marine food chains. Univ. Calif.

———, AND ———. 1970*b*. The ecology of the plankton off La Jolla, California, in the period April through September 1967. Bull. Scripps Inst. Oceanogr. **17:** 89–103.

———, AND ———. 1976. Some consequences of distributional heterogeneity of phytoplankton and zooplankton. Limnol. Oceanogr. **21:** 784–796.

———, ———, F. M. H. REID, J. NAPP, AND E. F. STEWART. 1985. Vertical structure of nearshore plankton off southern California: A storm and a larval food web. Fish. Bull. **83:** 151–170.

NICHOLLS, A. G. 1933. On the biology of *Calanus finmarchicus*. 3. Vertical distribution and diurnal migration in the Clyde Sea area. J. Mar. Biol. Assoc. U.K. **19:** 139–164.

NIELSEN, T. G., AND K. RICHARDSON. 1989. Food chain structure in the North Sea plankton communities: Seasonal variations of the role of the microbial loop. Mar. Ecol. Prog. Ser. **56:** 75–87.

OHMAN, M. D., AND J. A. RUNGE. 1994. Sustained fecundity when phytoplankton resources are in short supply: Omnivory by *Calanus finmarchicus* in the Gulf of St. Lawrence. Limnol. Oceanogr. **39:** 21–36.

PAFFENHÖFER, G. A. 1971. Grazing and ingestion rates of nauplii, copepodids and adults of the marine planktonic copepod *Calanus helgolandicus*. Mar. Biol. **11:** 286–298.

PEDERSEN, G., AND K. TANDE. 1992. Physiological plasticity to temperature in *Calanus finmarchicus*. Reality or artefact? J. Exp. Mar. Biol. Ecol. **155:** 183–197.

PETERSON, W. T., P. TISELIUS, AND T. KIØRBOE. 1991. Copepod egg production, moulting and growth rates, and secondary production, in the Skagerrak in August 1988. J. Plankton Res. **13:** 131–154.

RADACH, G. 1980. Preliminary simulations of the phytoplankton and phosphate dynamics during FLEX '76 with a simple two-component model. "Meteor" Forsch. Ergeb. Ser. A **22:** 151–163.

———. 1983. Simulations of phytoplankton dynamics and their interactions with other system components during FLEX '76, p. 584–610. *In* J. Sündermann and W. Lenz [eds.], North Sea dynamics. Springer.

———, J. BERG, B. HEINEMANN, AND M. KRAUSE. 1984. On the relation of primary production to grazing in the northern North Sea during the Fladen Ground Experiment (FLEX '76), p. 597–625. *In* M. J. R. Fasham [ed.], Flows of energy and materials in marine ecosystems: Theory and practice. Plenum.

———, AND A. MOLL. 1993. Estimation of the variability of production by simulating annual cycles of phytoplankton in the central North Sea. Prog. Oceanogr. **31:** 339–419.

RUNGE, J. A. 1985. Egg production rates of *Calanus finmarchicus* in the sea off Nova Scotia. Ergeb. Limnol. **21:** 33–40.

———. 1988. Should we expect a relationship between primary production and fisheries? The role of copepod dynamics as a filter of trophic variability. Hydrobiologia **167/168:** 61–71.

STEELE, J. H., AND E. W. HENDERSON. 1976. Simulation of vertical structure in a planktonic ecosystem. Scott. Fish. Res. Rep. **5:** 1–27.

TANDE, K. S. 1982. Ecological investigations on the zooplankton community of Balsfjorden, northern Norway: Generation cycles and variation in body weight and body content of carbon and nitrogen related to overwintering and reproduction in the copepod *Calanus finmarchicus* (Gunnerus). J. Exp. Mar. Biol. Ecol. **62:** 129–142.

THOMPSON, B. M. 1982. Growth and development of *Pseudocalanus elongatus* and *Calanus* sp. in the laboratory. J. Mar. Biol. Assoc. U.K. **62:** 359–372.

VIDAL, J. 1980. Physioecology of zooplankton. 1. Effects of phytoplankton concentration, temperature and body size on the growth rate of *Calanus pacificus* and *Pseudocalanus*. Mar. Biol. **56:** 111–134.

WILLIAMS, R., AND D. V. P. CONWAY. 1980. Vertical distribution of *Calanus finmarchicus* and *C. helgolandicus* (Crustacea: Copepoda). Mar. Biol. **60:** 57–61.

———, AND J. A. LINDLEY. 1980*a, b*. Plankton of the Fladen Ground during FLEX '76. 1. Spring development of the plankton community. 3. Vertical distribution, population dynamics and production of *Calanus finmarchicus* (Crustacea: Copepoda). Mar. Biol. **57:** 73–78; **60:** 47–56.

WROBLEWSKI, J. S., AND J. G. RICHMANN. 1987. The nonlinear response of plankton to wind mixing events—implications for survival of larval northern anchovy. J. Plankton Res. **9:** 103–123.

Submitted: 2 June 1993
Accepted: 13 February 1995
Amended: 28 October 1995